International Communications in Heat and Mass Transfer 133 (2022) 105956

Contents lists available at ScienceDirect

International Communications in Heat and Mass Transfer

journal homepage: www.elsevier.com/locate/ichmt

Numerical investigation of thermocapillary convection instability for large Prandtl number nanofluid in rectangular cavity

Xiaoming Zhou [a], Faxuan Chi [a], Yanni Jiang [a,*], Qisheng Chen [b]

[a] College of Mechanical and Electrical Engineering, Hohai University, Changzhou, China
[b] Institute of Mechanics, Chinese Academy of Sciences, Beijing, China

ARTICLE INFO

Keywords:
Nanofluid
Thermocapillary convection
Oscillatory flow
Critical Marangoni number

ABSTRACT

Oscillation characteristics and evolution process of large Prandtl number ($Pr = 58$) nanofluid thermocapillary convection is first reported in this work, and the variation of critical Marangoni number and flow instability under different nanoparticle concentrations is revealed. The results show that, nanofluid thermocapillary oscillatory convection consists of multiple vortices and these vortices migrate periodically from cold wall to hot wall, meanwhile, periodic temperature wave and stream function fluctuation cell exist in the oscillation process. As nanoparticle volume fraction increases, the critical Marangoni number decreases obviously, the oscillatory amplitude first increases and then decreases, and the oscillatory period almost increases linearly. This discovery can effectively promote the active control of thermocapillary convection instability.

1. Introduction

Thermocapillary convection is caused by thermal Marangoni effect at liquid free surface, and this flow exists in many industrial processes and occasions, so the flow transition and instability mechanism has been extensively investigated [1–7]. Since Choi [8] first raised the concept of nanofluid, the nanofluid has been used in many occasions. Nanofluid is a complex fluid and can be prepared by uniformly dispersing nanoparticle in liquid solvent. At present, nanofluid thermocapillary convection extensively exists in heat pipe, biomedicine, boiling heat transfer and other fields [9–13]. Therefore, the flow characteristics and instability of nanofluid thermocapillary convection have attracted many researchers' attention. Aminfar et al. [14] investigated the nanofluids thermocapillary-buoyancy convection in a float zone for the first time, and the computational results indicate that the increment of nanofluid concentration can influence the flow pattern. *Al* Sharafi et al. [15] investigated the flow pattern of nanofluid thermocapillary convection in droplet, and the heat transfer performance also is discussed. Saleh and Hashim [16] performed numerical study on thermocapillary flow in small aspect ratio cavity, and analyzed the effect of *Ma* number on the flow. Kolsi et al. [17] studied the steady-state buoyancy and thermocapillary convection entropy generation distribution and flow characteristics, the results show that as nanoparticle ratio increases the thermal transport increases. The authors [18] investigated the steady-state thermal capillary convection of nanofluids and revealed the influence of nanoparticle on thermocapillary convection. Sheikholeslami et al. [19] studied the effect of the magnetohydrodynamic effect on the nanofluid Marangoni convection. Abdullah et al. [20] applied a vertical temperature difference to the thin liquid layer, analyzed the linear stability of its nanofluid Marangoni convection. Gevorgyan et al. [21] investigated the speed evolution of the flow driven by Marangoni effect when the laser heated the surface of nanofluid. Zhuang and Zhu [22] studied the entropy production of buoyancy and Marangoni convection in porous medium region, and discussed the effect of nanoparticle concentration on entropy production. Recently, some researchers [23–43] further studied nanofluid surface tension induced flow, and the influence of nanoparticle on surface tension was considered.

The existing research works are mainly focus on the steady flow pattern of nanofluid thermocapillary convection, however, up to now there is still no report on flow instability, especially on the transient oscillation characteristics. It is well known that, nanofluid is a two-phase mixture fluid and its macroscopic physical properties are different from that of the base fluid, e.g. dynamic viscosity and thermal conductivity. Meanwhile, the Brownian motion of nanoparticle enhances the energy and momentum transfer between the fluid and nanoparticle. Then the flow transition condition and instability characteristics of nanofluid thermocapillary convection may different from that of single-phase fluid, and these problems need to be revealed for promote the application of nanoparticle in the active control of thermocapillary flow. So, the

* Corresponding author.
E-mail address: ynjiang@hhu.edu.cn (Y. Jiang).

https://doi.org/10.1016/j.icheatmasstransfer.2022.105956

Available online 7 March 2022
0735-1933/© 2022 Elsevier Ltd. All rights reserved.

Nomenclature

C_p	specific heat
h	height
l	length
Ma	Marangoni number
Nu	Nusselt number
P	pressure
Pr	Prandtl number
T	fluid temperature
t	time
$\vec{V}$	velocity vector
u, v	x, y-direction velocity
x, y	x, y-direction coordinate

Greek symbols

λ	thermal conductivity
ν	kinematic viscosity
μ	dynamic viscosity
ρ	density
τ	oscillatory period

Subscripts

f	fluid
nf	nanofluid
p	nanoparticle
h	hot wall
c	cold wall

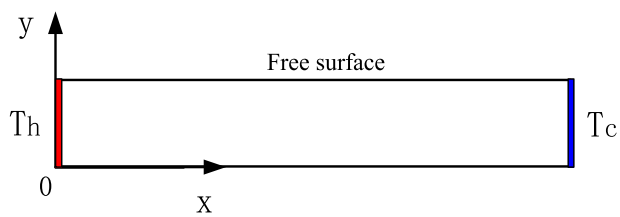

Fig. 1. Geometrical configuration and coordinate axes.

aim of the article is to reveal the nanofluid thermocapillary convection instability, and the influence of nanoparticles concentration on critical temperature difference and flow characteristics are also illustrated.

2. Equations and boundary conditions

Fig. 1 delineate a rectangular cavity filled with silicone oil, and the size is 20 mm (l) x 3 mm(h). The cavity is differentially heated at horizontal direction, and the temperatures at the left wall is T_h, and that of right wall is T_c ($T_h > T_c$). The bottom wall and free surface are assumed to be thermal adiabatic. In order to investigate the oscillatory instability, a small temperature difference is used to ensure the flow is laminar. The physical properties of silicon oil remain unchanged. Since there are conflicting views on the influence of nanoparticle on surface tension, here we just consider that surface tension varies linearly with temperature. Due to the depth of liquid layer is very small the buoyancy effect is ignored in our investigation. The initial temperature and flow fields in the cavity are $T = T_c$ and $\vec{V}$=0, respectively. Then, the governing equations of the thermocapillary convection of the nanofluid in cavity is [44–46]:

$$\nabla\cdot\vec{V} = 0\nabla\cdot\left(\rho_{nf,}\vec{V}_{nf}\right) = 0 \tag{1}$$

$$\frac{\partial\vec{V}}{\partial t} + \vec{V}\cdot\nabla\vec{V} = -\frac{1}{\rho_{nf}}\nabla p + \frac{\mu_{nf}}{\rho_{nf}}\nabla^2\vec{V} \tag{2}$$

Table 1
Thermophysical parameters [51].

Thermal properties component	ρ(kg/m^3)	μ(m^2/s)	λ(W/m K)	c_p(J/kgK)	γ_T(N/m K)
Silicon oil	910	0.455 × 10^{-3}	0.11	1400	−6.4 × 10^{-5}
Nanoparticles (Copper)	8978	/	387.6	381	/

$$\frac{\partial T}{\partial t} + \vec{V}\cdot\nabla T = \frac{\lambda_{nf}}{\rho_{nf}cp_{nf}}\nabla^2 T \tag{3}$$

where μ is dynamic viscosity, ρ is density, λ is thermal conductivity, t is time, p is pressure, $\vec{V}$ is velocity vector and T is temperature, and the subscript *nf* denotes nanofluid.

2.1. Physical properties of fluid

The measurement of nanofluid physical properties is of great significance. The equations of density and specific heat are written as:

$$\rho_{nf} = \alpha_p\rho_p + (1-\alpha_p)\rho_f \tag{4}$$

$$(\rho cp)_{nf} = \alpha_p(\rho c_p)_p + (1-\alpha_p)(\rho c_p)_f \tag{5}$$

The Eq. (4) is the density equation of nanofluid, according to the mixing rule proposed in literature [47]. The Eq. (5) is specific heat expression, which is according to the hypothesis of the thermal balance [48].

Thermal conductivity of nanofluid [49]:

$$\lambda_{nf} = \lambda_f\left[\frac{(\lambda_p + 2\lambda_f) - 2\alpha_p(\lambda_f - \lambda_p)}{(\lambda_p + 2\lambda_f) + \alpha_p(\lambda_f - \lambda_p)}\right] \tag{6}$$

Dynamic viscosity of nanofluid [50]:

$$\mu_{nf} = \frac{\mu_f}{(1-\alpha_p)^{2.5}} \tag{7}$$

where α_p is nanoparticle volume fraction.

2.2. Boundary conditions

$$u = v = 0, T = T_c \text{ as } x = 0 \tag{8}$$

$$u = v = 0, T = T_h \text{ as } x = l \tag{9}$$

$$u = v = 0, \frac{\partial T}{\partial y} = 0 \text{ as } y = 0 \tag{10}$$

$$\mu\frac{\partial u}{\partial y} = -\gamma_T\frac{\partial T}{\partial x}, v = 0, \frac{\partial T}{\partial y} = 0 \text{ as } y = h \tag{11}$$

Marangoni numbers: $Ma = \frac{|\gamma_T|\Delta TL}{\mu\alpha}$.

Nusselt number: $\mathrm{Nu} = -\frac{\lambda_{nf}}{\lambda_f}\cdot\left(\frac{\partial T}{\partial x}\cdot\frac{L}{T_h - T_c}\right)$

Average Nusselt number: $\mathrm{Nu}_{ave} = \frac{1}{h}\cdot\int_0^h Nu(y)dy$

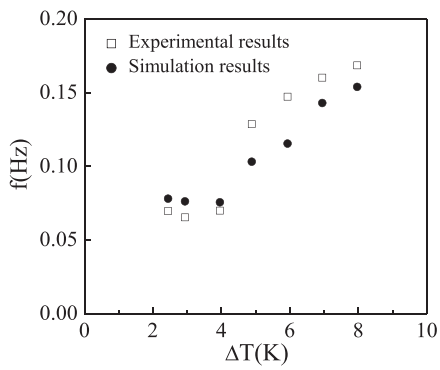

Fig. 2. Comparison of oscillatory frequency with Schwabe [52].

Table 2
Average oscillatory period under different grids ($\alpha_p = 0.05$ and $Ma = 1.17 \times 10^6$).

Grid numbers	Average oscillatory period (s)
100 × 30	12.91
150 × 40	12.61
200 × 50	12.50
250 × 70	12.47

2.3. Thermophysical parameters of nanofluid

In this study, the base fluid is silicon oil and the nanoparticle is copper. Table 1 shows the physical properties of the base solution and nanoparticles.

3. Solution method

The governing equations are solved by Fluent, in which the diffusion term is discretized by second order central difference scheme, and the convection term is discretized by the QUICK format. Solve pressure-velocity coupling problem with PISO algorithm. In the process of numerical calculation, the solution is considered to be converge as the relative variation rate of temperature, velocity and pressure is smaller than 10^{-5}. The comparison with experimental result of Schwabe [52] is given in Fig. 2, the correctness of the computation is verified. Moreover, the effectiveness of the code also can refer to our previous papers [53,54]. The mesh used is non-uniform orthogonal grid, which is refined near all walls and free surface. Grids of 100 × 30, 150 × 40, 200 × 50 and 250 × 70 are tested, and the average oscillatory period under different grids is illustrated in Table 2. The local stream function distribution under different meshes is given in Fig. 3, the structure of vortex

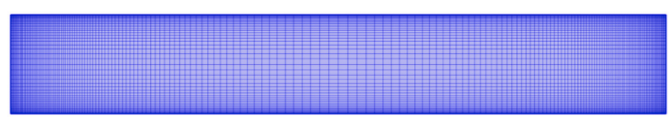

Fig. 4. Grid distribution.

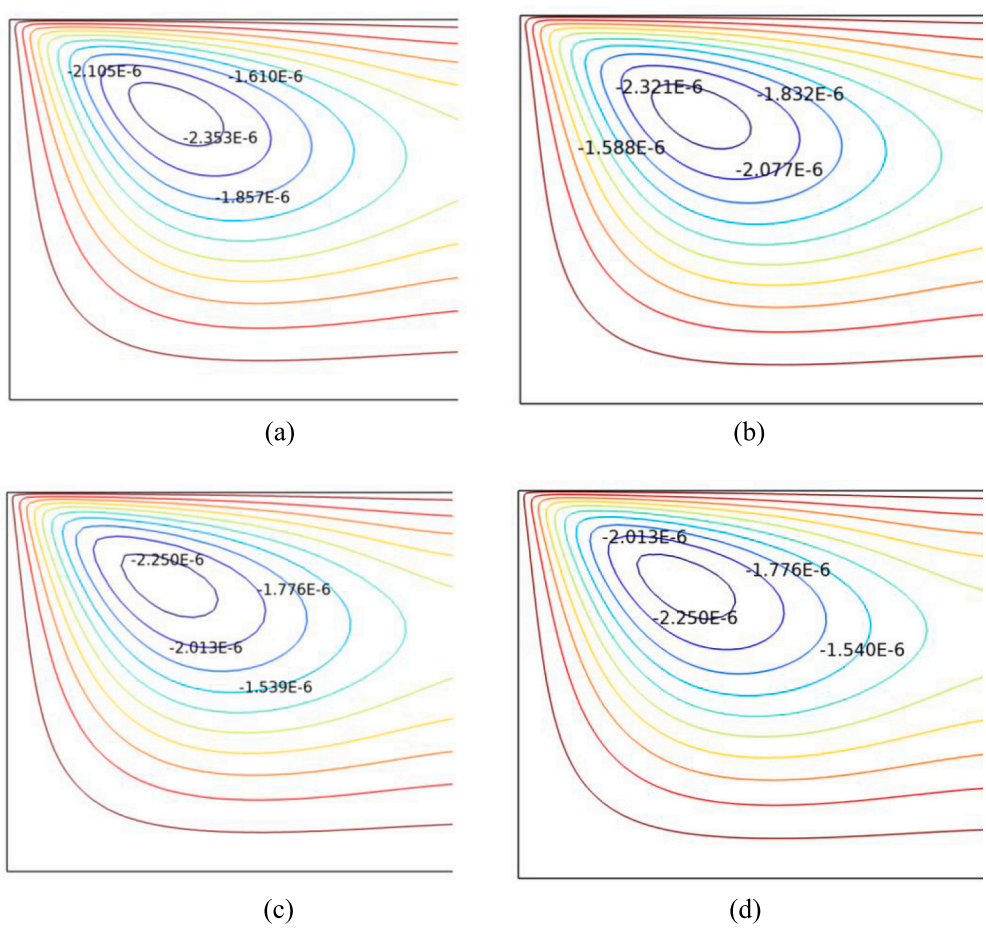

Fig. 3. Stream function distribution under different grids as $Ma = 1.17 \times 10^6$ and $\alpha_p = 0.02$ ((a) 100 × 30, (b) 150 × 40, (c) 200 × 50, (d) 250 × 70).

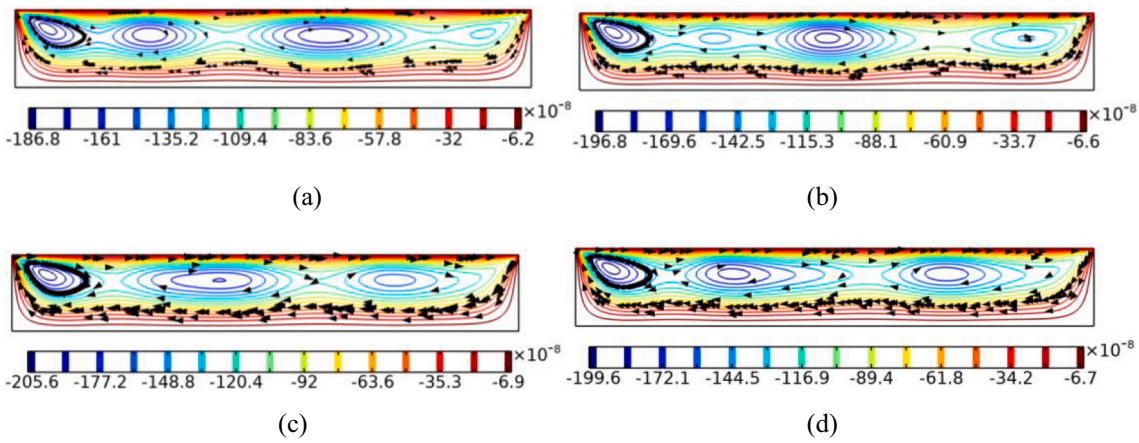

Fig. 5. Vortices evolution during one oscillatory period as $Ma = 1.17 \times 10^6$ and $\alpha_p = 0.02$ ((a) t = t', (b) t = t' + τ/4, (c) t = t' + τ/2, (d) t = t' + 3τ/4).

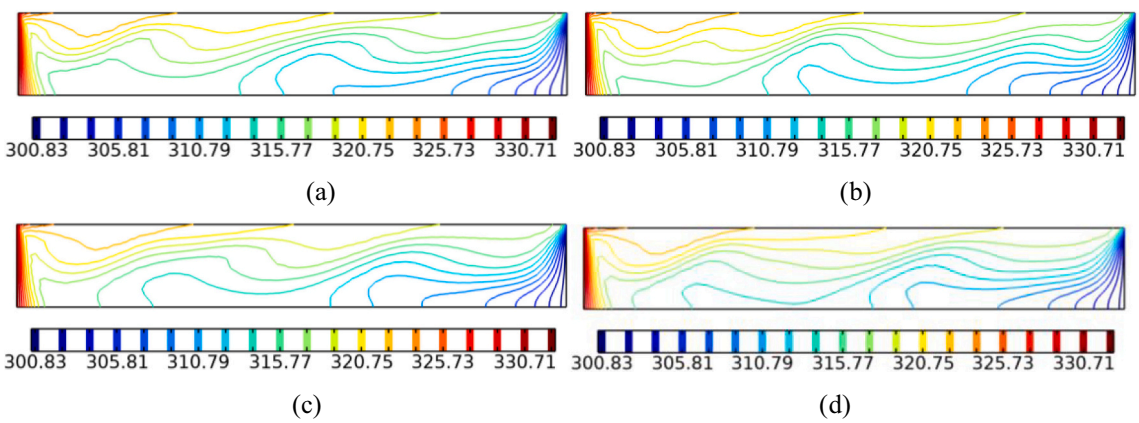

Fig. 6. Temperature field evolution during one oscillatory period as $Ma = 1.17 \times 10^6$ and $\alpha_p = 0.02$ ((a) t = t', (b) t = t' + τ/4, (c) t = t' + τ/2, (d) t = t' + 3τ/4).

is the same and the value tends to be constant. Therefore, the mesh 200 × 50 is suitable in this paper, and the mesh is shown in Fig. 4.

4. Results and discussions

When Marangoni number of the system is lower than critical Marangoni number (Ma_{cri}), a steady large vortex will be formed. As Ma number increases, the thermocapillary flow transitions from steady state to oscillatory mode. In particular, when *Ma* number is greater than Ma_{cri}, Ma_{cri} is about 1.08×10^6 as $\alpha_p = 0.02$, the flow field disturbance appears at the right side. As Marangoni number further increases, the periodic migration vortex will appear in the whole cavity. Fig. 5 shows the vortices evolution during one oscillatory period as $Ma = 1.17 \times 10^6$ and $\alpha_p = 0.02$, in which t = t' is the starting time of oscillation period and τ is one period. We can see that a fixed vortex located at the vicinity of the left wall, and the structure remains unchanged. However, at the central and right side region the convective vortices exist periodic reciprocating migration, and there are multiple flow patterns in the evulotion process, such as the generation, merging, and migration. Moreover, the vortex generates at the corner of free surface and the right wall, and travels from the right to the left. This indicates the disturbance energy from thermocapillary force. The corresponding temperature contours distribution is shown in Fig. 6, in which the isotherms indicates a periodic migration, namely the temperature contours structure from the left moves to the right gradually. In particuar, the isotherms pattern on the left remains basically stable, while the dense isotherms structure in the central region gradually migrates to the right side periodically. Moreover, the number and position of the dense isotherms structure are consistent with that of vortex, this indicates the coupling relationship between macro flow field and temperature field in the oscillatory thermocapillary convection.

In order to indicates the detailed oscillation characteristics of nanofluid thermocapillary convection, the evolution history of temperature and velocity of monitoring point (x = 10 mm,y = 3 mm) at free surface is shown in Fig. 7, in which (b) and (d) are the partial enlarged view of (a) and (c), respectively. We can see that the temperaure and velocity value of monitoring point manifests a periodic oscillation, and the phase difference of temperature and velocity is about τ/2. The reason is that the convection is induced by temperature gradient and the velocity oscillation lags behind temperature oscillation.

In order to further demonstrate the disturbance characteristics of temperature field and flow field, the fluctuations of temperature and stream function are defined as the difference between the instantaneous value and its time-averaged value, e.g., $\omega'(x, y, t) = \omega(x, y, t) - \omega_0(x, y)$, where $\omega'(x, y, t)$ is the temperature or stream function fluctuation and $\omega_0(x, z) = \frac{1}{\tau'}\int_0^{\tau'} \varphi(x, y, t)dt$ is the time-averaged value, $\tau'$is the time length much larger than the oscillation period [55]. Fig. 8 gives the temperature fluctuation evolution during one oscillatory period as $Ma = 1.17 \times 10^6$ and $\alpha_p = 0.02$, we can see that temperature wave appear in the whole liquid layer, and migrates from the right side to the left side. The temperature fluctuation originates from the right wall, the fluctuation intensity first increases and then decreases during traveling process, and finally disappears at the vicinity of the left wall. Moreover, in the process of temperature wave propagation, the positive and negative value deviations appear alternately.

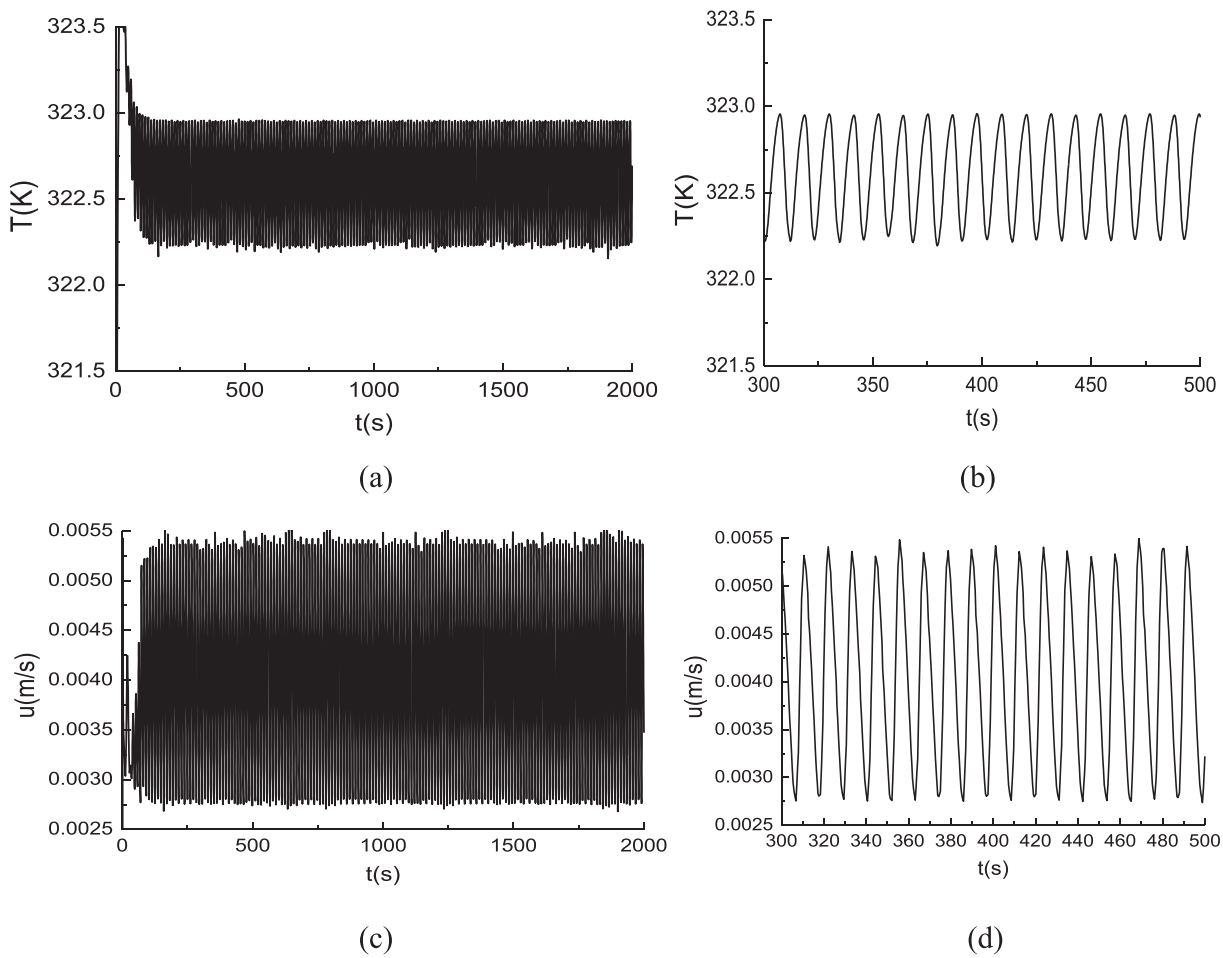

Fig. 7. Time evolution history of temperature ((a) and partial enlarged view (b)) and velocity ((c) and partial enlarged view (d)) at monitoring point as $Ma = 1.17 \times 10^6$ and $\alpha_p = 0.02$.

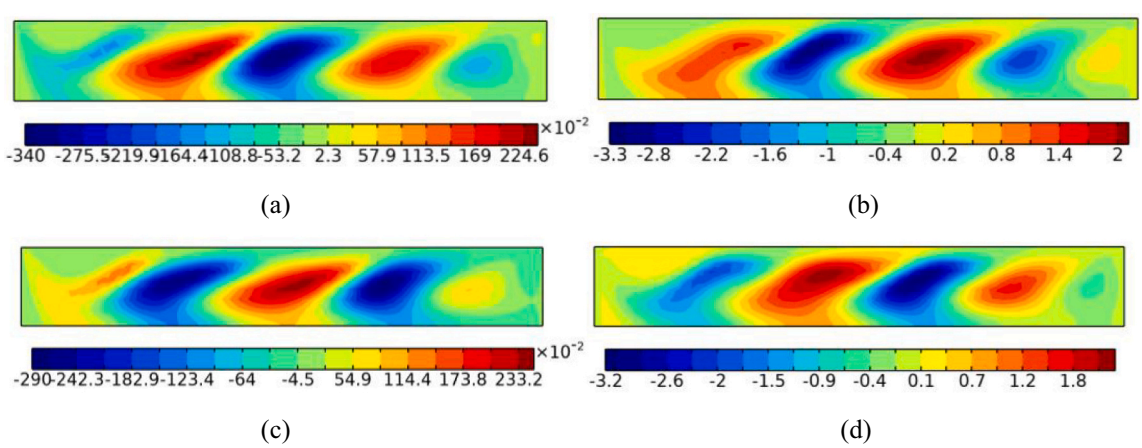

Fig. 8. Temperature fluctuation evolution during one oscillatory period as $Ma = 1.17 \times 10^6$ and $\alpha_p = 0.02$ ((a) t = t', (b) t = t' + τ/4, (c) t = t' + τ/2, (d) t = t' + 3τ/4).

The evolution of stream function fluctuation during one oscillation period is shown in Fig. 9. It can be seen that the stream function fluctuation field is composed of multiple fluctuation cells, in which the positive and negative fluctuation values appear alternately and moves from the right to the left side. Moreover, the fluctuation cell also originates at the right wall and disappears at the left wall, and in the migration process the intensity of fluctuation cell first increases, then decreases, and finally disappears. During the evolution process the number of fluctuation cell changes periodically, meanwhile, the structure size and strength of fluctuation cells also change accordingly.

Fig. 10 indicates the variation of critical *Ma* of thermocapillary convection with volume fraction of nanoparticles. It shows that M_{cri} of singe-phase fluid is obvious larger than that of nanofluid, this means that nanofluid thermocapillary convection is more prone to instability. This

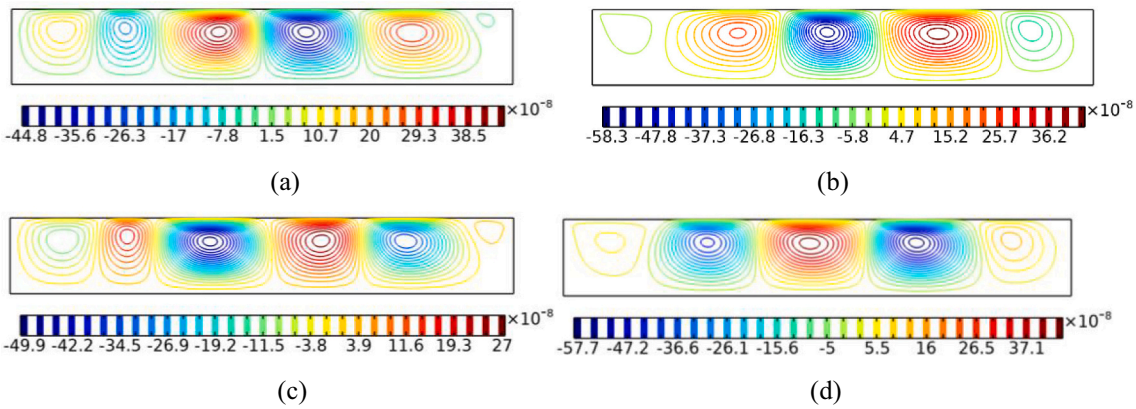

Fig. 9. Stream function fluctuation evolution during one oscillatory period as $Ma = 1.17 \times 10^6$ and $\alpha_p = 0.01$ ((a) t = t', (b) t = t' + τ/4, (c) t = t' + τ/2, (d) t = t' + 3τ/4).

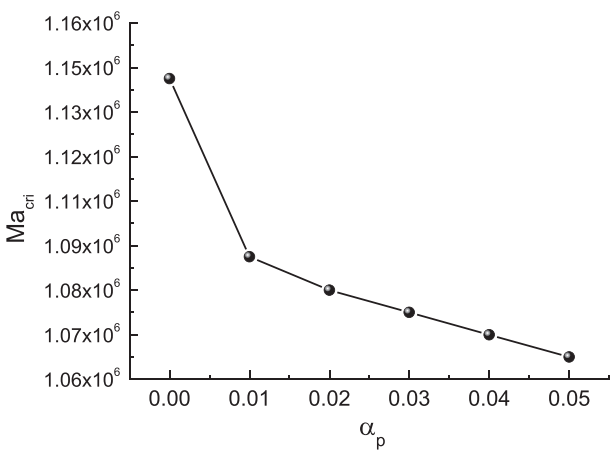

Fig. 10. Variation of Ma_{cri} with α_p.

is due to the variation of the thermal physical properties, namely the addition of nanoparticles results in the increase of dynamic viscosity and thermal conductivity, then the heat transfer strengthens but the momentum diffusion rate decreases, so the flow become unstable under smaller Marangoni number. Moreover, as nanoparticle volume fraction increases the critical Marangoni number linearly deceases gradually. This variation trend provides an effective method to predict the instability critical parameter of nanofluid thermocapillary convection.

Fig. 11 gives temperature fluctuation distribution under different nanoparticles volume fractions as $Ma = 1.17 \times 10^6$. From Fig. 8 we can know that, the temperature fluctuation value is variable during one oscillatory period, so here the temperature fluctuation field distributions are given at the time as the monitoring point temperature is at the peak. The results show that the temperature fluctuation field of single-phase fluid is different from that of nanofluid, in which the core of positive and negative disturbance waves is not located on a horizontal line, this indicates the disturbance energy gradient exists in both horizontal and vertical directions. The temperature fluctuation field distribution shows the same pattern with different volume fractions of nanoparticle. This indicates the nanoparticle concentration can affect the thermocapillary convection instability, but the influence is weaker. Moreover, with volume fraction increasing the range of temperature fluctuation changes, but the change trend is not monotonous. The corresponding stream function fluctuation under different nanoparticle concentrations is given in Fig. 12. As $\alpha_p = 0$, the stream function fluctuation field exists seven independent cells, in which the cell locates at the central region is negative and the other cells are positive, and this fluctuation mode is different from that of nanofluid thermocapillary convection. Similar to that of temperature deviation, as volume fraction of nanoparticle increases the change of the stream function fluctuation range is also nonmonotonous. Moreover, as volume fraction of nanoparticle varies from 0.01 to 0.05, the whole structure of stream function fluctuation cells is basically the same, however, at the vicinity of left wall the stream function fluctuation cell enhanced slightly and a new cell appears.

Fig. 13 gives the time history of velocity oscillation at monitoring

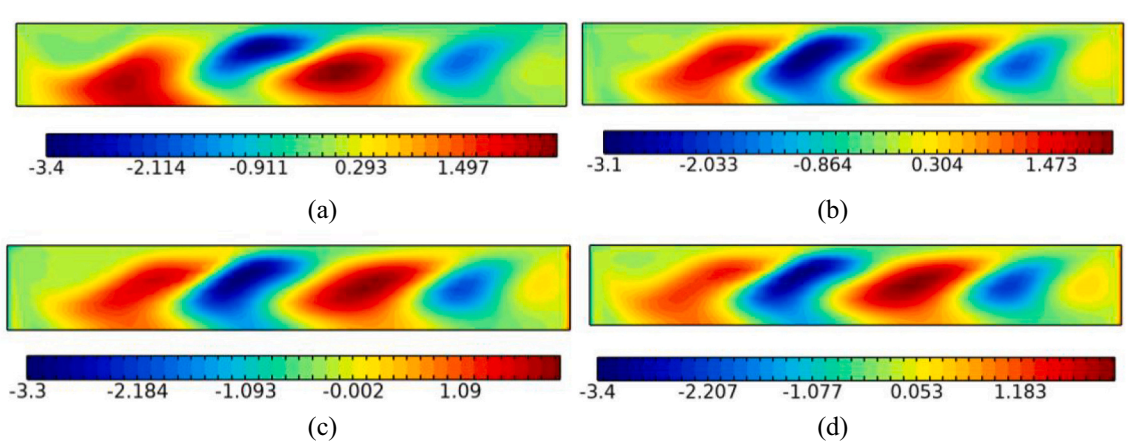

Fig. 11. Temperature fluctuation distribution under different nanoparticles volume fractions as $Ma = 1.17 \times 10^6$ ((a) $\alpha_p = 0$, (b) $\alpha_p = 0.01$, (c) $\alpha_p = 0.03$, (d) $\alpha_p = 0.05$).

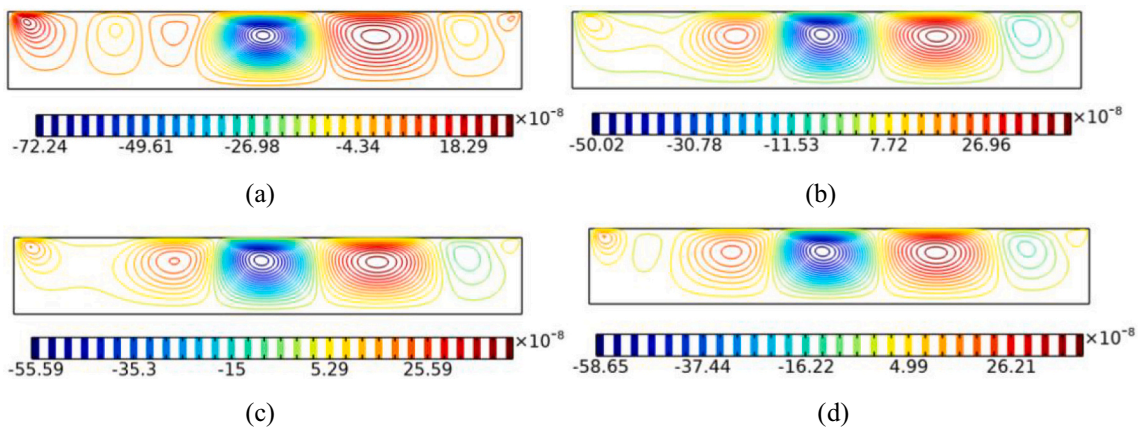

Fig. 12. Evolution of stream function fluctuation with nanoparticle volume fraction as $Ma = 1.17 \times 10^6$ ((a) $\alpha_p = 0$, (b) $\alpha_p = 0.01$, (c) $\alpha_p = 0.03$, (d) $\alpha_p = 0.05$).

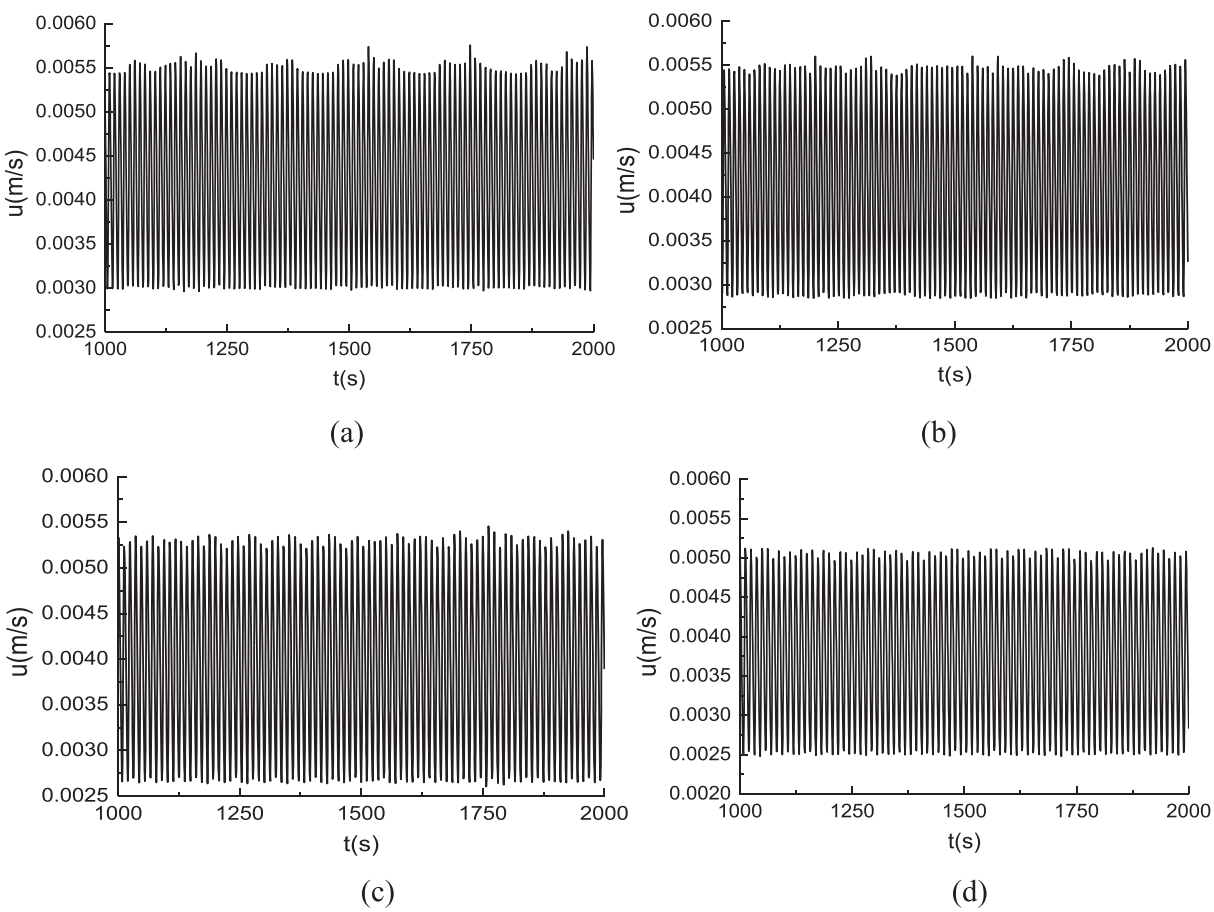

Fig. 13. Time history of velocity oscillation at monitoring point under different nanoparticle concentrations as $Ma = 1.17 \times 10^6$ ((a) $\alpha_p = 0$, (b) $\alpha_p = 0.01$, (c) $\alpha_p = 0.03$, (d) $\alpha_p = 0.05$).

point (x = 10 mm, y = 3 mm) under different nanoparticle concentrations as $Ma = 1.17 \times 10^6$. The results show that under different nanoparticle vonlume fractions the velocity evolution history at monitoring point demonstrates the similar oscillation characteristics, however, the velocity oscillation range deceases and the oscillatory period increases slightly. In particularly, the maximum velocity decreases from 0.0055 m/s at $\alpha_p = 0$ to 0.0051 m/s at $\alpha_p = 0.05$, and the minimum velocity from 0.003 m/s decreases to 0.0025 m/s.

In order to show the detailed change of oscillation characteristics, Fig. 14 gives the variation of average velocity oscillatory amplitude and period at monitoring point with nanoparticle volume fraction as $Ma = 1.17 \times 10^6$. As $\alpha_p = 0$, the oscillatory amplitude is obvious smaller than that of nanofluid thermocapillary convection, this shows that the addition of nanoparticle can effectively improve the oscillation amplitude of thermocapillary convection. However, as nanoparticle concentration increases the velocity oscillation amplitude diminishes gradually, this is due to the increase of fluid viscosity inhibits fluid oscillation. Fig. 14(b) exhibits that as volume fraction of nanoparticle varises from 0 to 0.05,

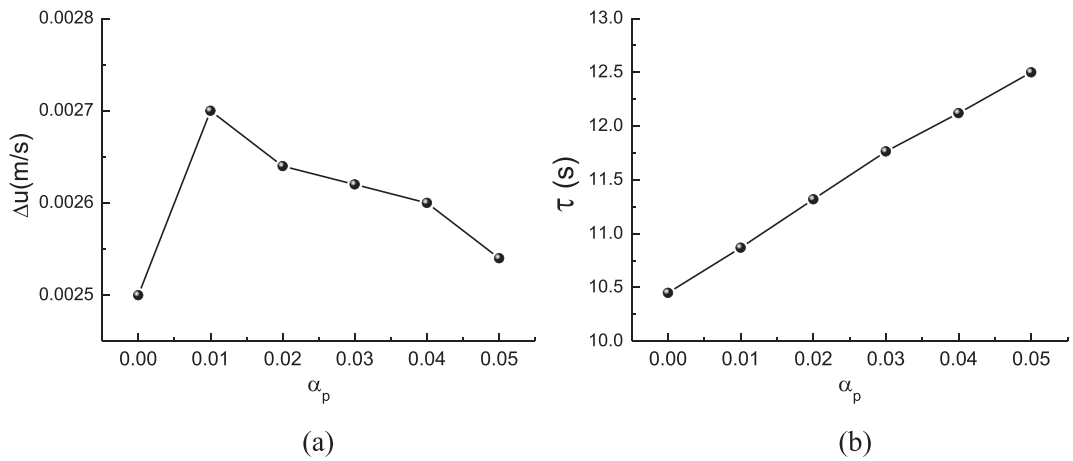

Fig. 14. Variation of average velocity oscillatory amplitude (a) and period (b) at monitoring point with nanoparticle volume fraction as $Ma = 1.17 \times 10^6$.

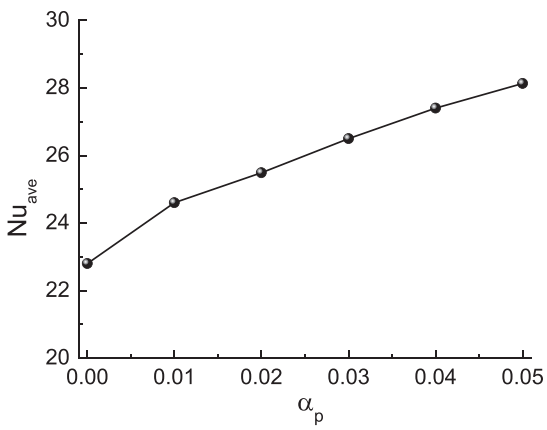

Fig. 15. Nu_{ave} at the left wall versus α_p.

the oscillatory period of nanofluid thermocapillary flow almost increases linearly. This variation trend indicates that the oscillatory characteristics of thermocapillary convection can be adjusted by the addtion of nanoparticles, and the choice of appropriate nanoparticle concentration is important.

Fig. 15 shows the variation of Nu_{ave} at the left wall with α_p, in which Nu_{ave} increases with α_p increasing. This indicates that the heat transfer between the nanofluid and the left wall enhances with α_p increasing. That is due to the increment of thermal conductivity enhances the heat transfer.

5. Conclusions

Thermocapillary convection of large *Pr* number nanofluid in cavity is numerically investigated, and the oscillatory characteristics under different nanoparticle concentrations are analyzed. Detailed conclusions are listed below:

1) For nanofluid oscillatory thermocapillary convection, the flow field consists of multiple convective cells, and these convective cells migrate periodically from the right to the left side. Meanwhile, there are periodic temperature wave and stream function fluctuation cell traveling.
2) As volume fraction of nanoparticle increases, the critical Marangoni number deceases gradually, the velocity oscillatory amplitude first increases and then decreases, and the oscillatory period almost increases linearly.
3) The oscillatory characteristics of thermocapillary convection can be adjusted by the addtion of nanoparticles, and the choice of appropriate nanoparticle concentration is important.

CRediT authorship contribution statement

Xiaoming Zhou: Conceptualization, Methodology, Software. **Faxuan Chi:** Data curation. **Yanni Jiang:** Supervision. **Qisheng Chen:** Writing – review & editing.

Declaration of Competing Interest

We declare that we have no financial and personal relationships with other people or organizations that can inappropriately influence our work, there is no professional or other personal interest of any nature or kind in any product, service and/or company that could be construed as influencing the position presented in, or the review of, the manuscript entitled, “Numerical investigation of thermocapillary convection instability for large Prandtl number nanofluid in rectangular cavity”.

Acknowledgments

The work was supported by National Natural Science Foundation of China (No. 12102128, 51976080), the Fundamental Research Funds for the Central Universities (No. B200201037).

References

[1] J.J. Yu, D.F. Ruan, Y.R. Li, et al., Experimental study on thermocapillary convection of binary mixture in a shallow annular pool with radial temperature gradient, Exp. Thermal Fluid Sci. 61 (2015) 79–86.
[2] J.J. Yu, Y.R. Li, C.M. Wu, et al., Three-dimensional thermocapillary-buoyancy flow of a binary mixture with Soret effect in a shallow annular pool, Int. J. Heat Mass Transf. 90 (2015) 1071–1081.
[3] W.Y. Shi, K.Y. Tang, J.N. Ma, et al., Marangoni convection instability in a sessile droplet with low volatility on heated substrate, Int. J. Therm. Sci. 117 (2017) 274–286.
[4] S. Yang, R. Liang, S. Xiao, et al., Influence of ambient airflow on free surface deformation and flow pattern inside liquid bridge with large prandtl number fluid (Pr>100) under gravity, J. Heat Transf. 139 (12) (2017), 122001.
[5] X.M. Zhou, Z.G. Liu, X.L. Huai, Evolution of free surface in the formation of thermo-solutocapillary convection within an open cavity, Microgr. Sci. Technol. 28 (4) (2016) 421–430.
[6] X.M. Zhou, X.L. Huai, Thermo-solutocapillary convection in open rectangular cavity with dynamic free surface, ASME J. Heat Transf. 137 (082901) (2015) 1–9.
[7] X.M. Zhou, X.L. Huai, Free surface deformation of thermo-solutocapillary convection in axisymmetric liquid bridge, Microgr. Sci. Technol. 27 (2015) 39–47.
[8] U.S. Choi, Enhancing thermal conductivity of fluids with nanoparticles, ASME FED 231 (1995) 99–103.
[9] M. Susanta, Thermocapillary flow of thin cu-water nanoliquid film during spin coating process, Int. Nano Lett. 7 (1) (2017) 9–23.

[10] D.S. Wu, J.L. Huang, L. Kong, et al., Coupled mechanisms of arc, weld pool and weld microstructures in high speed tandem TIG welding, Int. J. Heat Mass Transf. 154 (2020), 119641.
[11] K.G. Naveen, K.T. Arun, K.G. Subrata, Heat transfer mechanisms in heat pipes using nanofluids-a review, Exp. Thermal Fluid Sci. 90 (2018) 84–100.
[12] W. Du, J. Zhao, H. Li, Y. Zhang, J. Wei, K. Li, Thermal dynamics of growing bubble and heat transfer in microgravity pool boiling, in: W. Hu, Q. Kang (Eds.), Physical Science under Microgravity: Experiments on Board the SJ-10 Recoverable Satellite. Research for Development, Springer, 2019, pp. 73–99.
[13] A.Z. Stetten, S.V. Iasella, T.E. Corcoran, S. Garoff, T.M. Przybycien, R.D. Tilton, Surfactant-induced Marangoni transport of lipids and therapeutics within the lung, Curr. Opin. Coll. Interf. Sci. 36 (2018) 58–69.
[14] H. Aminfar, M. Mohammadpourfard, F. Mohseni, Numerical investigation of thermocapillary and buoyancy driven convection of nanofluids in a floating zone, Int. J. Mech. Sci. 65 (1) (2012) 147–156.
[15] A. Al-Sharafi, A.Z. Sahin, B.S. Yilbas, et al., Marangoni convection flow and heat transfer characteristics of water-CNT nanofluid droplets, Num. Heat Transf. Part A: Appl. 69 (7) (2016) 763–780.
[16] H. Saleh, I. Hashim, Buoyant Marangoni convection of nanofluids in square cavity, Appl. Math. Mech. 36 (9) (2015) 1169–1184.
[17] L. Kolsi, E. Lajnef, W. Aich, et al., Numerical investigation of combined buoyancy-thermocapillary convection and entropy generation in 3D cavity filled with Al_2O_3 nanofluid, Alexandr. Eng. J. 56 (1) (2017) 71–79.
[18] Y.N. Jiang, Z. Xu, Numerical investigation of nanofluid thermocapillary convection based on two-phase mixture model, Microgravity Sci. Tech. 29 (5) (2017) 365–370.
[19] M. Sheikholeslami, A.J. Chamkha, Influence of Lorentz forces on nanofluid forced convection considering Marangoni convection, J. Mol. Liq. 225 (2017) 750–757.
[20] A.A. Abdullah, S.A. Althobaiti, K.A. Lindsay, Marangoni convection in water-alumina nanofluids: dependence on the nanoparticle size, Europ. J. Mech. B Fluids 67 (2018) 259–268.
[21] G.S. Gevorgyan, K.A. Petrosyan, R.S. Hakobyan, et al., Experimental investigation of Marangoni convection in nanofluids, J. Contemp. Phys. (Armenian Acad. Sci.). 52 (4) (2017) 362–365.
[22] Y.J. Zhuang, Q.Y. Zhu, Analysis of entropy generation in combined buoyancy-Marangoni convection of power-law nanofluids in 3D heterogeneous porous media, Int. J. Heat Mass Transf. 118 (2018) 686–707.
[23] Y.N. Jiang, X.M. Zhou, Analysis of flow and heat transfer characteristics of nanofluids surface tension driven convection in a rectangular cavity, Int. J. Mech. Sci. 153-154 (2019) 154–163.
[24] Qingang Xiong, Ahmad Hajjar, Bader Alshuraiaan, et al., State-of-the-art review of nanofluids in solar collectors: a review based on the type of the dispersed nanoparticles, J. Clean. Prod. 310 (2021), 127528.
[25] M. Izadi, B. Bastani, M.A. Sheremet, 2020a. Numerical simulation of thermogravitational energy transport of a hybrid nanoliquid within a porous triangular chamber using the two-phase mixture approach, Adv. Powder Technol. 31 (6) (2020) 2493–2504.
[26] Mohsen Izadi, Mohammad Ghalambaz, S.A.M. Mehryan, Location impact of a pair of magnetic sources on melting of a magneto-Ferro phase change substance, Chin. J. Phys. 65 (2020) 377–388.
[27] Mohsen Izadi, Effects of porous material on transient natural convection heat transfer of Nano-fluids inside a triangular chamber, Chin. J. Chem. Eng. 28 (5) (2020) 1203–1213.
[28] S.A.M. Mehryan, AliTahmasebi, MohsenIzadi, MohammadGhalambaz, melting behavior of phase change materials in the presence of a non-uniform magnetic-field due to two variable magnetic sources, Int. J. Heat Mass Transf. 149 (2020), 119184.
[29] G.K. Ramesh, S.A. Shehzad, Mohsen Izadi, Thermal transport of hybrid liquid over thin needle with heat sink/source and darcy-forchheimer porous medium aspects, Arab. J. Sci. Eng. 45 (2020) 9569–9578.
[30] MohsenIzadi Shu-RongYan, Mikhail A. Sheremet, et al., Inclined Lorentz force impact on convective-radiative heat exchange of micropolar nanofluid inside a porous enclosure with tilted elliptical heater, Int. Commun. Heat Mass Transf. 117 (2020), 104762.
[31] S.A.M. Mehryan, Mohammad Ghalambaz, Reza Kalantar Feeoj, et al., Free convection in a trapezoidal enclosure divided by a flexible partition, Int. J. Heat Mass Transf. 149 (2020), 119186.
[32] M. Hojjat, S.Gh. Etemad, R. BagheriaJ, Thibault, rheological features of non-Newtonian nanofluids flows induced by stretchable rotating disk, Int. Commun. Heat Mass Transf. 38 (2) (2011) 144–148.
[33] S.A. Shehzad, Mohammed SaadKamel BaderAlshuraiaan, et al., Influence of fin orientation on the natural convection of aqueous-based nano-encapsulated PCMs in a heat exchanger equipped with wing-like fins, Chem. Eng. Process. Process Intensif. 160 (2021), 108287.
[34] Hasan Sajjadi, Natural convection heat transfer in a porous cavity with sinusoidal temperature distribution using Cu/water nanofluid: double MRT Lattice Boltzmann method, Commun. Comput. Phys. 29 (1) (2022) 292–318.
[35] A. Amiri Deloueia, H. Sajjadia, R. Mohebbib, M. Izadi, Experimental study on inlet turbulent flow under ultrasonic vibration: pressure drop and heat transfer enhancement, Ultrason. Sonochem. 51 (2019) 151–159.
[36] M. Izadi, M.M. Shahmardan, A. Behzadmehr, et al., Modeling of effective thermal conductivity and viscosity of carbon structured nanofluid, Challeng. Nano Micro Scales 3 (1) (2015) 1–13.
[37] M. Izadi, M.M. Shahmardan, A.M. Rashidi, Study on thermal and hydrodynamic indexes of a nanofluid flow in a micro heat sink, Trans. Phenom. Nano Micro Scales 1 (1) (2013) 53–63.
[38] Qingang Xiong, Sam Altnji, Tahar Tayebi, A comprehensive review on the application of hybrid nanofluids in solar energy collectors, Sustain. Energy Technol. Assessm. 47 (2021), 101341.
[39] Mohsen Izadi, Mamdouh El Haj Assad, Use of nanofluids in solar energy systems, design perform, Optimiz. Renew. Energy Syst. (2021) 221–250.
[40] Qingang Xiong, Tahar Tayebic, Mohsen Izadi, Numerical analysis of porous flat plate solar collector under thermal radiation and hybrid nanoparticles using two-phase model, Sustain. Energy Technol. Assessm. 47 (2021), 101404.
[41] B. Ahmadrez, Shahrestani, Bader Alshuraiaan, MohsenIzadi, combined natural convection-FSI inside a circular enclosure divided by a movable barrier, Int. Commun. Heat Mass Transf. 126 (2021), 105426.
[42] Qingang Xiong, Hashim M. Alshehri, Rezvan Monfaredi, Application of phase change material in improving Trombe Wall efficiency: an up-to-date and comprehensive overview, Energy Build. 258 (2022), 111824.
[43] Mohsen Izadi, Mikhail Sheremet, Hashim M. Alshehri, et al., Numerical study on charging process inside a grid-structure thermal storage, J. Energy Stor. 45 (2022), 103522.
[44] M.K. Smith, S.H. Davis, Instabilities of dynamic thermocapillary liquid layers. 1. Convective instabilities, J. Fluid Mech. 132 (7) (1983) 119–144.
[45] H.C. Kuhlmann, S. Albensoeder, Three-dimensional flow instabilities in a thermocapillary-driven cavity, Phys. Rev. E 77 (2008), 036303-1–036303-15.
[46] Peng Zhu, Li Duan, Qi Kang, Transition to chaos in thermocapillary convection, Int. J. Heat Mass Transf. 57 (2013) 457–464.
[47] S.K. Das, S.U.S. Choi, W. Yu, T. Pradeep, Nanofluids Science and Technology, John Wiley & Sons, Hoboken, New Jersey, 2008.
[48] K. Khanafer, K. Vafai, A critical synthesis of thermophysical characteristics of nanofluids, Int. J. Heat Mass Transf. 54 (2011) 4410–4428.
[49] R.L. Hamilton, O.K. Crosser, Thermal conductivity of heterogeneous two component systems, Ind. Eng. Chem. Fundam. 1 (3) (1962) 187–191.
[50] H.C. Brinkman, The viscosity of concentrated suspensions and solutions, J. Chem. Phys. 20 (4) (1952) 571.
[51] Maxim Teitela, Dietrich Schwabe, Yu. Alexander, Gelfgat, experimental and computational study of flow instabilities in a model of Czochralski growth, J. Cryst. Growth 310 (2008) 1343–1348.
[52] D. Schwabe, S. Benz, Thermocapillary flow instabilities in an annulus under microgravity -results of the experiment MAGIA, Adv. Space Res. 29 (2002) 629–638.
[53] Y.N. Jiang, X.M. Zhou, Analysis of flow and heat transfer characteristics of nanofluids surface tension driven convection in a rectangular cavity, Int. J. Mech. Sci. 153-154 (2019) 154–163.
[54] H.L. Huang, X.M. Zhou, The impact of normal magnetic fields on instability of thermocapillary convection in a two-layer fluid system, ASME J. Heat Transf. 131 (2009) 1–7.
[55] K. Li, B. Xun, W.R. Hu, Some bifurcation routes to chaos of thermocapillary convection in two-dimensional liquid layers of finite extent, Phys. Fluids 28 (2016), 054106.